geosciences

MDPI

Article

Geophysical and Geological Views of Potential Water Resources in the North-Eastern Adriatic Sea

Michela Giustiniani [1,*], Martina Busetti [1], Michela Dal Cin [1], Erika Barison [1], Aurélie Cimolino [2], Giuseppe Brancatelli [1] and Luca Baradello [1]

[1] National Institute of Oceanography and Applied Geophysics—OGS, Borgo Grotta Gigante 42/C, 34010 Sgonico, Trieste, Italy; mbusetti@inogs.it (M.B.); mdalcin@inogs.it (M.D.C.); ebarison@inogs.it (E.B.); gbrancatelli@inogs.it (G.B.); lbaradello@inogs.it (L.B.)

[2] Independent Researcher, Via Dei Platani 14, 33052 Cervignano, Udine, Italy; aureliecimolino@tiscali.it

* Correspondence: mgiustiniani@inogs.it

Abstract: The increasing demand for freshwater requires the identification of additional and less-conventional water resources. Amongst these, offshore freshwater systems have been investigated in different parts of the world to provide new opportunities to face increasing water requests. Here we focus on the north-eastern Adriatic Sea, where offshore aquifers could be present as a continuation of onshore ones. Geophysical data, in particular offshore seismic data, and onshore and offshore well data, are interpreted and integrated to characterise the hydrogeological setting via the interpretation of seismo-stratigraphic sequences. We focus our attention on two areas located in the proximity of the Tagliamento and Isonzo deltas. Well and seismic data indicate that the Quaternary sediments, that extend from onshore to offshore areas, are the most promising from an offshore freshwater resources point of view, while the several kilometres thick pre-Quaternary carbonate and terrigenous sequences likely host mainly salty waters.

Keywords: offshore aquifers; north-eastern Adriatic Sea; seismic data; wells

Citation: Giustiniani, M.; Busetti, M.; Dal Cin, M.; Barison, E.; Cimolino, A.; Brancatelli, G.; Baradello, L. Geophysical and Geological Views of Potential Water Resources in the North-Eastern Adriatic Sea. *Geosciences* **2022**, *12*, 139. https://doi.org/10.3390/geosciences12030139

Academic Editors: Helder I. Chaminé and Jesus Martinez-Frias

Received: 18 February 2022
Accepted: 11 March 2022
Published: 18 March 2022

1. Introduction

Recently, the interest in offshore-freshened groundwater has been growing very fast because of the rising demand for potable water, related to population and economic growth, especially in the emerging countries, and the strong effects of climate change on this resource. In fact, in several regions, groundwater resources are under strong stress because of their depletion or contamination, e.g., [1]. The presence of these important reserves of fresh or brackish waters (with total dissolved solids < 10 g/L; [2]) have been already documented in many continental margins around the world, e.g., [3–7]. Many authors have proposed an estimate of the global volume of this resource on the order of 105 to 106 km^3 [2,8,9], even if these estimates are affected by high uncertainties because of the paucity of information about this resource. The offshore-freshened waters are mainly hosted in siliciclastic and carbonate sediments, with variable ages, mainly deposited during the Cenozoic, e.g., [2]. These resources can be located at a distance greater than 100 km from the shoreline and at 4.5 km depth from the seafloor [2]. Five mechanisms have been proposed to explain the genesis of the offshore-freshened groundwater, e.g., [10]. A mechanism could be related to the present active connection between onshore and offshore aquifers due to the presence of continuous confined aquifers or/and geological heterogeneity due to topographic gradients, e.g., [11–14]. The second one is related to the maximum glacial period, during which the sea level reached the lowest values, allowing for the exposure of the shelf, which was recharged with fresh and/or brackish water, also far from the present shoreline [2,9,15,16]. Other processes could be related to subglacial and proglacial injection, e.g., [16–23], to post-sedimentary alteration processes, e.g., [24,25] and to gas hydrates dissociation, e.g., [26].

In this context, the north-eastern Adriatic Sea is an interesting study area, where offshore aquifers may potentially be present and possibly connected with a multi-layered aquifer system located onshore [27,28]. This region hosts several kilometres thick Meso-Cenozoic carbonate sequences and a Cenozoic clastic succession that host semi-confined or confined aquifers. In addition, in the area, marine seismic lines have been acquired with different resolutions (Figure 1). These are an important tool to characterise offshore aquifers, as already demonstrated by several authors, e.g., [29]. In fact, seismic reflection data can contribute to identifying lithological changes related to environmental changes and sea level variations in the past and at a regional scale [29].

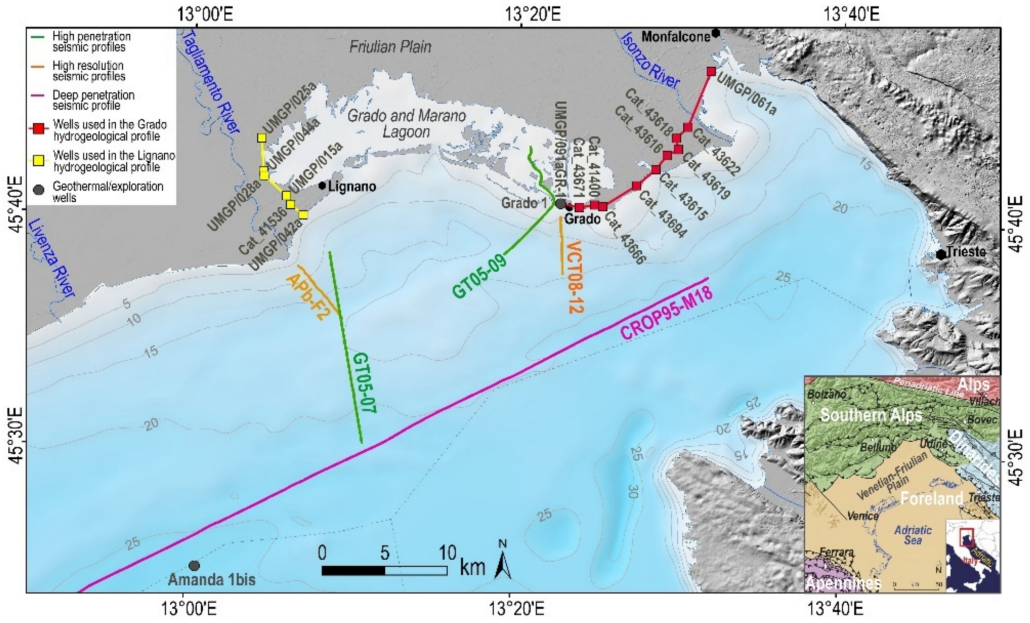

Figure 1. Location map of the study area over the Friulian Plain and the north-eastern Adriatic Sea. The analysed marine high penetration multichannel seismic reflection profiles acquired by the National Institute of Oceanography and Applied Geophysics (OGS) are represented in bold green lines, while the orange bold lines represent the OGS high-resolution seismic boomer profiles. The pink bold line shows the position of the deep crustal investigation multichannel seismic profile CROP95-M18. The positions of the Grado 1 geothermal well and of the Amanda 1bis exploration well are represented by the grey hexagons. The water wells used to construct the Lignano and Grado lithostratigraphical profiles of the aquifers are shown by yellow and red squares, respectively. Bathymetry in depth with cells of 50 m and contours every 5 m, gridding performed by [30] by using grids from Italy and Slovenia [31] and Croatia [32]. Digital Elevation Model compiled for Italy (5 and 10 m cells by [33,34], respectively), Slovenia (10 m cells; [35]) and Istria (25 m cells; [36]). The inset map shows the chains of the Alps, Apennines, Dinarides and relative foreland domain, together with the main tectonic structures [37–43]. Map compiled by using ArcGis® (ESRI, 2017) software; datum WGS84, projection UTM33.

The aim of this paper is to investigate the connection between onshore and offshore aquifers in the north-eastern Adriatic Sea, and specifically identify features related to the presence of the freshwater aquifers, and/or of layers hosting confined offshore paleo-aquifers, through the integration of well data and a high-penetration and high-resolution seismic dataset. We focused our attention on two areas, located in the offshore Tagliamento and Isonzo rivers, respectively (north-eastern Italy; Figure 1). As suggested by Reference [1], the deltaic areas are very interesting from a hydrogeological point of view, because rivers generate important thickness of sediments, especially in proximity to high mountains areas. In addition, as mentioned above, in the past, this region was characterised by changes in the sea level related to the glaciations, which probably influenced the connection between the onshore and offshore aquifers.

2. Geological and Hydrological Setting

The present northern Adriatic Sea-Northern Venetian-Friulian Plain area belonged to the same geological domain from the Late Paleozoic until the Early Jurassic rifting. At that time the area was differentiated in the structural paleogeographical units of the deep sea Belluno Basin on the west from those on the east, where during the Jurassic and Cretaceous the Friuli-Dinaric Carbonate Platform (FDCP) developed [44,45]. Approximately 1 kilometre thick of aggradational and progradational systems of FDCP were deposited [46,47] above 3–4 km of the Upper Triassic to Jurassic carbonate sequences. The sedimentation was not continuous and several episodes of subaerial exposure occurred mainly related to tectonic events: (i) in the Upper Jurassic with the development of huge karstic phenomena and red soil deposition; (ii) in the Lower Cretaceous with the development of an extensive erosional surface; (iii) in the Upper Cretaceous with erosional processes and the development of red soils at the top ([48] and references therein).

During the Paleocene, the ongoing westward propagation of the External Dinarides caused the drowning of the Cretaceous-Paleocene FDCP and the deposition within the foredeep of turbidites constituted by silty marls and sandstones (Trieste Flysch). Deep-sea carbonate marl and breccias of the Scaglia or Scaglia Alpina (Aptian-early Eocene) were deposited in the Belluno Basin and, subsequently, from the Middle Eocene to the Miocene, the basin was filled by the Gallare Marls.

In the Late Oligocene-Early/Middle Miocene with the development of the Southern Alps, the filling of the foreland started with the deposition of the terrigenous carbonate platform sequences of the Cavanella Group (Chattian-Langhian), and when the alpine chain propagated fast south-eastward, the foredeep was filled by up the clastic wedge of the Middle-Late Miocene Molassa ([49] and references therein).

At the end of the Miocene, a complex interplay between the sea level drop estimated in 800–900 m due to the Messinian Salinity Crisis of the Mediterranean Sea [50], and compressional tectonics produced the subaerial exposure of the area, with the development of a drainage system that produced several kilometres-long and several hundred meter deep canyons [46,47,51,52].

The Messinian erosion was followed by marine transgression with deposition of Pliocene-Middle Pleistocene marine sediments that include cycles from deep-marine clays and silts passing into shallower and sandier deposits of the Eraclea Sands, Santerno Clays and Asti Sands. The sedimentation of these sequences was interrupted by the late Zanclean tectonic uplift, which produced the Mid-Pliocene unconformity, and the drowning episodes during the Piacenzian and late Gelasian, the latest of which was responsible for the development of the Late Gelasian Surface [53–55].

The Middle-Late Pleistocene records the glacial/interglacial eustatic driven regression and transgression with alternation of continental and marine deposits, respectively. Eight cycles of marine ingressions and regressions occurred in the Middle-Late Pleistocene, with the first ice cap developed in the Alps about 800,000 years ago [56]. The periods of glacial maximum, with the development of the icecap over the Alps, favoured the maximum erosion rates within the mountain chain [57]. Sedimentation in the plain areas occurred due to river flooding with the construction of fans and megafans with the material coming from glacial erosion in the mountain chain areas. The main phases of the plain aggradation are those relating to the deglacial phases when the river flooding was greater [28]. The alluvial deposits relating to the glacial/cataglacial periods are mainly characterised by gravels and pebbles with a sandy matrix, with the oldest deposits that can be cemented. During the interglacial periods, in the northern Adriatic and the southern Venetian-Friulian Plain, the marine transgression caused the deposition of pelitic sands/sands related to coastal and deltaic environments, pelitic and fine sands related and lagoon environments with tidal influence, and silts and clays related to platform environments [49].

From a hydrogeological point of view, the main onshore aquifer system located in the Friulian Plan is hosted in the Plio-Quaternary sediments. It is relatively well characterised because of the availability of direct and indirect measurements, such as well information

and seismic data, e.g., [28,58–61]. A spring belt divides this plain into two parts: the upper and the lower Friulian Plain. The sediments of the upper Friulian Plain host a phreatic aquifer with a high capacity of storage water [58], while an aquifer system is present in the lower part. The spring belt is the result of extensive and abundant groundwater spills [28] because this feature separates two areas characterised by different permeability decreasing from north to south. In the lower plain, the aquifer system includes eleven artesian layers, named from "A" to "M", some of which are divided into two sub-layers (Figure 2; [28]), that show strong variability in depth and lateral continuity. The thicknesses of the aquifers, generally increase toward the SW but are also variable due to the tectonic and geological setting of the pre-Plio-Quaternary substrate. The fluid circulation is mainly due to primary porosity in these sediments, while in the pre-Plio-Quaternary terrigenous and carbonate sequences, the fluid circulation is related to secondary porosity due to fracturing and karstic conduits [62]. The upper eight aquifers are hosted in Plio-Quaternary sediments, while the deeper ones are presumably hosted in the underlying Miocene molasse and Paleogene flysch. These latter are characterised by thermal water with a high concentration of solutes and temperatures greater than 35 °C [28].

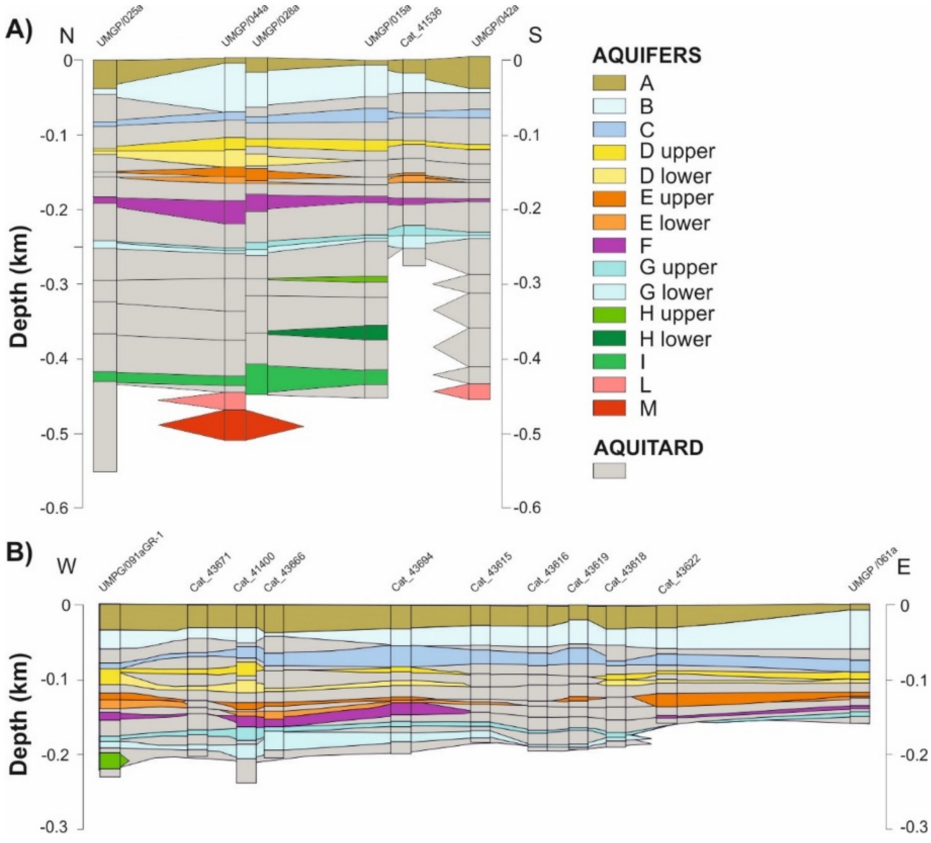

Figure 2. Correlation among the aquifers along the two selected profiles with directions N-S (Lignano profile) (**A**) and NE-SW (Grado profile) (**B**), respectively. The position of the two profiles N-S and NE-SW is reported in Figure 1 with yellow and red lines, respectively. The profiles were developed on the basis of available well information [28]. The grey layers represent the aquitard, while the other ones are the identified aquifers. The nomenclature of the aquifers is from [28].

The Amanda-1bis exploration wells drilled in the northern Adriatic Sea, down to 7280 m, revealed the several kilometres thick Triassic to Cretaceous carbonate sequence and the overlying 1 km Eocene to Pliocene terrigenous sediment contain salty and brackish waters [63] (Figure 1).

A low enthalpy aquifer (temperature ranging from 20 to 90 °C) is hosted in the Meso-Cenozoic carbonates and is considered an important geothermal reservoir. The Grado 1 well,

drilled in 2008, as a pilot borehole for the exploitation of this geothermal reservoir, revealed the occurrences of two main levels of low enthalpy aquifers in highly fractured Paleogene and Cretaceous carbonate layers with a temperature of about 44 °C (Figure 1; [61,64]). The geothermal reserve is constituted by fossil waters at high conductivity concentrated in the rock portion characterised by higher permeability, and with a porosity estimated to be about 8–10% [62]. These waters flow also in the vertical direction along fractures and karstic conduits. Natural resurgences of the low enthalpy salty water occur at the Roman Bath of Monfalcone at 32.6–39.8 °C, interpreted to be ancient diagenetically modified seawater [65], and along the Istrian coast in eight marine springs at 22–30 °C [66]. The geochemical characterization of one of them provides 5‰ of salinity consistent with mixing and advection of karstic groundwater from S-W Slovenia and seawater [67].

3. Materials and Methods

A geodatabase of geothermal and thermal-mineral resources of the Friuli Venezia Giulia region was developed in the frame of EERA GEOTERMIA-Project, among a collaboration between the University of Trieste and OGS [68]. The database contains: (a) literature information; (b) results of several projects having different purposes, including hydrocarbon exploration, groundwater and geothermal resources characterisation; (c) available data, such as geophysical data, in particular seismic lines; (d) information about more than 600 onshore boreholes. For each well, lithological, hydrogeological and/or geochemical information are available.

Some wells drilled for oil&gas exploration are publicly available through ViDEPI [63]. For the present study, we considered the exploration well Amanda 1bis, drilled in the northern Adriatic Sea in 1979 by ENI-AGIP, INA Naftapline, SIR and ELF oil companies and reaches a depth up to 7305 m below sea level [63], and the Grado 1 well drilled in 2008 for the investigation, and eventually exploitation, of the geothermal reservoir [63,64]. These exploration wells provide information about the aquifers hosted in the several kilometres thick sedimentary sequence, but unfortunately, they have no information from the surface to about 300/500 m depth. Instead, the characterization of the aquifers hosted in the upper several hundred metres depth comes from wells drilled for water supply purposes.

To assist in the identification of features linked to the presence of aquifers imaged in marine seismic sections, we considered isobath and isopach maps for each identified aquifer located in the Friulian Plain and developed by [28] by using a geostatistical approach considering the onshore 603 boreholes, selected from more than 3000 boreholes [28]. In addition, we developed two profiles, which represent the correlation among the confined aquifers, on the basis of available boreholes (Figure 2). As shown in Figure 1, one profile is parallel to the Tagliamento river with an approximate N-S direction, while the second one has a SW-NE direction, ending in the proximity of Grado, westward of the Isonzo mouth. In our study, we used marine seismic lines with different resolutions. To image the overall sedimentary sequences up to several kilometres depth, we used regional multichannel seismic data acquired in the north-eastern Adriatic Sea calibrated by an offshore exploration well. We considered the marine CROP95-M18 ultra-high penetration multichannel seismic profile (Figure 3) acquired by OGS with the R/V OGS Explora in 1995 and belonging to the "CROsta Profonda" (Deep Crust) Italian project (a joint venture between CNR "National Research Council", ENI-AGIP "Italian Oil Company" and ENEL "Italian National Electricity Authority"), aiming at deep crustal investigation [69,70]. This low-resolution seismic line, recently reprocessed in time and depth domain [71], is NE-SW oriented across the northern Adriatic Sea and it is calibrated by the Amanda 1bis exploration well, located at about two kilometres south-westward from the line (Figure 1). The high penetration seismic data were acquired by OGS with the R/V OGS Explora in 2005 by using airgun arrays, as a seismic source, and a 600 m seismic streamer with 48 channels for profile GT05-07 (Figure 4), while the line GT05-09 was acquired through the lagoon by using a 120 m seismic streamer with 12 channels (Figure 5; [46]).

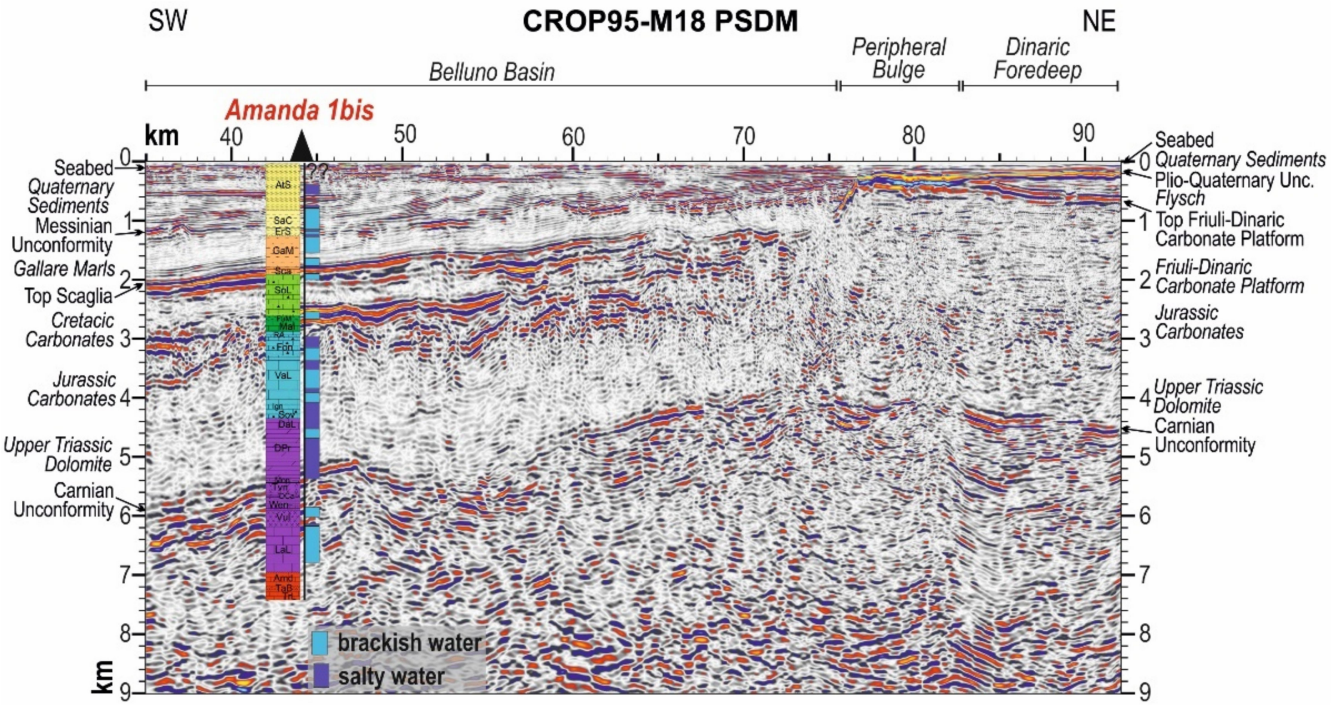

Figure 3. Pre-stack depth migrated [71] seismic profile CROP95-M18. The Amanda 1bis exploration well [63], drilled up to 7280 m, is located about 2 km south-westward. Its stratigraphy calibrates the seismic: the thick carbonate sequence is composed of Meso-Cenozoic carbonates, whose top deepens SW-ward up to 3 km depth in the Belluno Basin. Here, they are covered by the Eocene-Miocene Gallare Marls. In correspondence of the peripheral bulge, in front of the Grado Island, the carbonates of the Friuli-Dinaric Carbonate Platform raise up to 600 m and deepen NE-ward in the Dinaric foredeep domain filled by the Eocene Flysch. The top of the Eocene-Miocene terrigenous units is depicted by Messinian Unconformity due to sea level drop. This unconformity is in turn buried under Pliocene progradation eroded at the top by Mid-Pliocene Unconformity, in the Belluno Basin; whereas in the eastern part of the area erosion lasted until Mid-Pleistocene. The Plio-Quaternary marine and continental deposits drape the shallowest part of the sedimentary sequence. The well lithostratigraphic units are: Asti Sands (AtS, Quaternary), Santerno Clays (SaC, Lower Pliocene), Eraclea Sands (ErS, Lower Pliocene), Gallare Marls (GaM, Eocene), Scaglia Alpina (Sca, Paleocene), Soccher Limestone (SoL, Upper Cretaceous), Marne a Fucoidi Formation (FuM, Lower Cretaceous), Maiolica (Mai, Lower Cretaceous), Rosso Ammonitico superiore (RA, Upper Jurassic), Fonzaso Formation (Fon, Upper Jurassic), Vajont Limestone (VaL, Middle Jurassic), Igne Formation (Ign, Lower Jurassic), Soverzene Formation (Sov, Lower Jurassic), Dachstein Limestone (DaL, Upper Triassic), Dolomia Principale (DPr, Upper Triassic), Monticello Formation (Mon, Upper Triassic), Trevenanzes Formation (Tvn, Upper Triassic), Dolomia Cassiana (DCa, Upper Triassic), Wengen Formation (Wen, Middle Triassic), Vulcanite (Vul, Middle Triassic), Latemar Limestone (LaL, Middle Triassic), Amanda Formation (Amd, Permian), Tarvisio Breccia (TaB, Permian), Trogkofel Limestone (TrL, Permian).

To characterise the uppermost sedimentary sequences, we used two high-resolution seismic datasets acquired by OGS in 2000, in the offshore of the Tagliamento mouth, and 2006 in the offshore of Grado, close to the Isonzo mouth, using as source an electro-dynamic plate UWAK 05 Nautik connected with PULSAR 2002 CEA and a mono-channel streamer (an eight-element hydrophone array) (Figure 6; [31]).

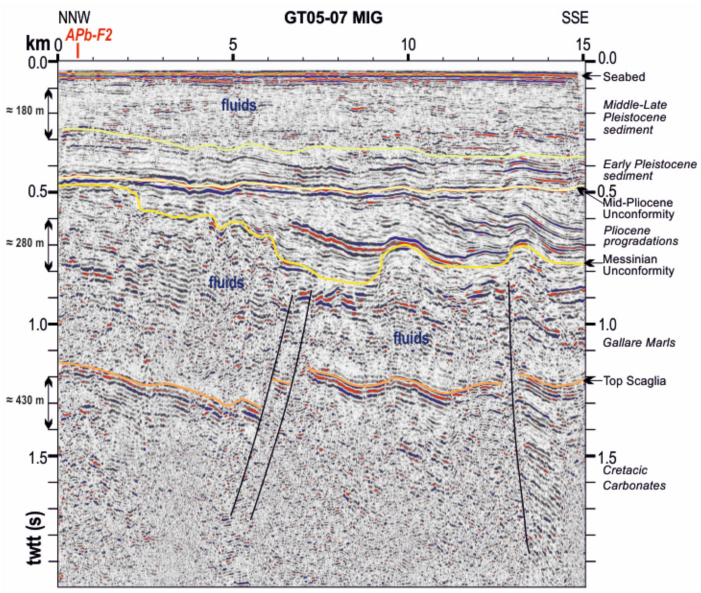

Figure 4. High penetration multichannel time migrated seismic profile GT05-07, offshore the Tagliamento river delta. The seismic profile shows the sedimentary sequence composed of Meso-Cenozoic carbonates of the Belluno Basin, buried under the Eocene-Miocene Gallare Marls. These at the top are depicted by the Messinian Unconformity, covered by Pliocene progradations, which are in turn cut by the Mid-Pliocene Unconformity. Early Pleistocene marine progradation sediments seal the entire sequence, which in turn are covered by the alternation of continental and marine Middle-Late Pleistocene sediment. Along the vertical scale of the profile, the approximate correspondent thickness of 0.2 s twt (two way time) in meters is reported, calculated by using mean P-wave velocity values (obtained by tomographic analysis; [72–75]), of 1750 m/s, 2800 m/s and 4300 m/s for the Plio-Quaternary sediments, Eocene-Miocene deposits and Meso-Cenozoic carbonates, respectively. The seismic image shows presence of fluids within the sedimentary sequence.

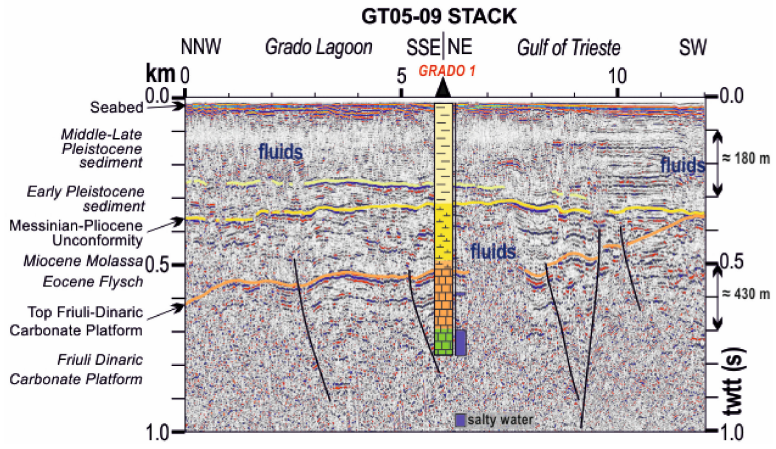

Figure 5. High penetration multichannel seismic profile GT05-09, offshore the Grado Island. The seismic shows the sedimentary sequence composed by the Meso-Cenozoic Friuli-Dinaric Carbonate Platform, buried under the Eocene flysch and Miocene Molassa, depicted by the Messinian-Pliocene Unconformity. Pleistocene sediments seal the entire sequence. The stratigraphy of the Grado 1 geothermal well [64,76], 0.5 km SE of the profile, is represented on the seismic profile. Depths are converted into twt by using mean P-wave velocity values obtained from tomographic analysis; [72–75]: 1750 m/s for the Pleistocene sediments (light yellow block), 2800 m/s for the terrigenous deposits of Molassa and Flysch (golden yellow and orange blocks, respectively), 4300 m/s for Lower Eocene-Paleocene and Cretaceous carbonates (orange and green blocks) containing two deep aquifers with salty waters. The seismic image shows the presence of fluids within the sedimentary sequence.

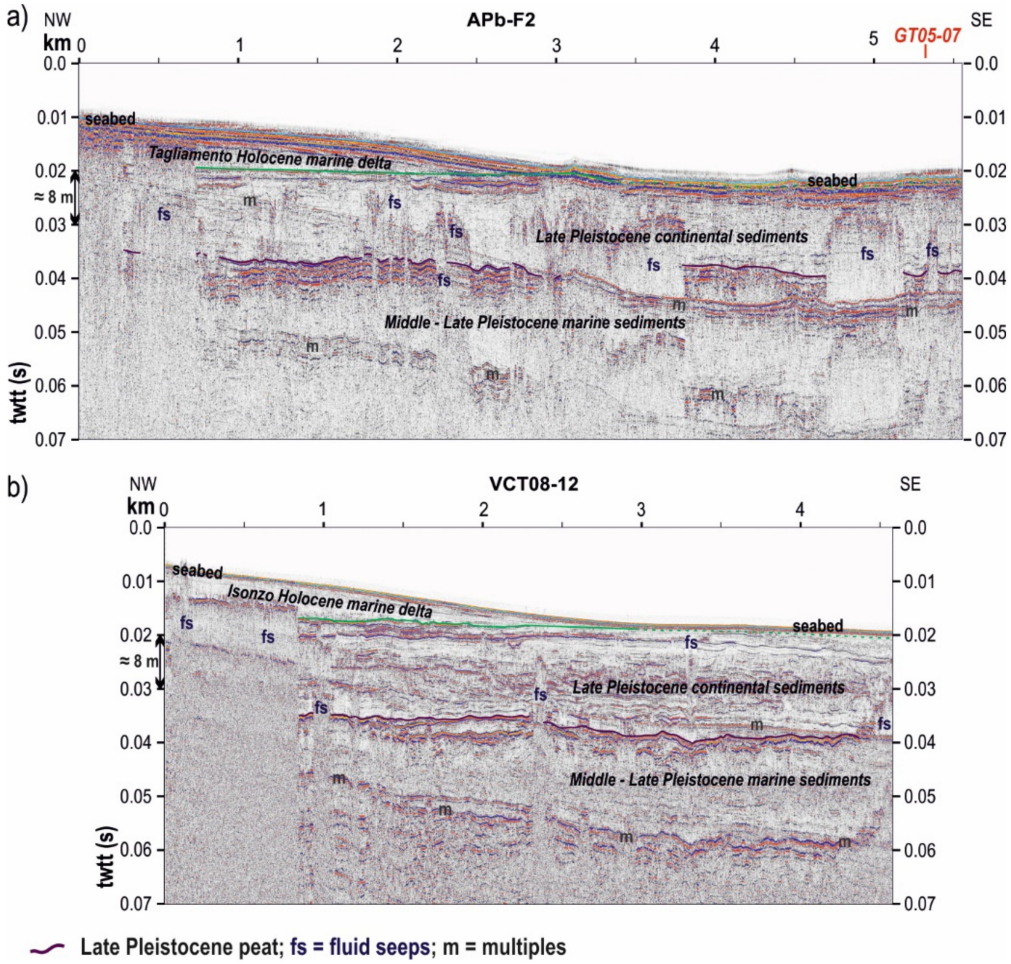

Figure 6. Marine high-resolution boomer profiles APb-F2 (**a**) and VCT08-12 (**b**) offshore the Tagliamento river delta and Grado Island, respectively. The seismic sections show the sedimentary sequence composed of Middle-Late Pleistocene and Holocene marine and continental sediments whose deposition was influenced by the cyclic variations of the sea level in relation to glacial and interglacial phases. The Middle-Late Pleistocene marine sediment related to the Thyrrenian marine transgression (125 ka), are covered in turn by Late Pleistocene continental sediments, characterized by the channel levee system that deposited during the last glacial period in the fluvial plane environment, that may host the shallower aquifer A and possibly aquifer B. The sediments are draped by the prograding Holocene delta front and pro-delta of the Tagliamento and Isonzo rivers, related to the last marine transgression phase. Along the vertical scale of the profiles is reported the approximated correspondent thickness of 0.01 s twt in meters, calculated by using mean P-wave velocity value (obtained through tomographic analysis; [72–75]) of 1750 m/s for the Quaternary sediments. The seismic images show the presence of fluids within the sedimentary sequence. Multiple reflections, related to the seabed and sub-bottom horizons with strong reflection coefficient, mask primary signal in the deeper part of the seismic sections.

4. Results

The interpretation of the seismic lines was focused on identifying the main sedimentary sequences hosting the aquifers, with particular regard to features that may support the possible continuation of aquifers offshore and/or the presence of trapped water in offshore sediments.

Two hydrogeological profiles were developed in the southern Friulian Plain close to the coast, by using water well information, with N-S and NE-SW directions, respectively. The two profiles show that the aquifers are not continuous and have a variable thickness and depth across the Friulian Plain (Figure 2). This strong lateral variability confirms that

aquifers are preferentially hosted in sediments showing changes in lithological characteristics. In addition, the well information confirms the presence of the aquifers in proximity to the coast, supporting the hypothesis of the continuation of the aquifers system offshore.

The interpretation of the seismic profiles calibrated by the well information, allows to identify the following main seismo-stratigraphic units and their inferred hydrogeological characteristics:

(a) The several kilometres thick Upper Triassic-Paleogene carbonate sequences host water characterised by variable salinity, from brackish to salty. The multichannel seismic profile CROP95-M18, calibrated with the Amanda 1bis well, indicates that: (a) the Middle Triassic carbonates, occurring below 4.5–7.5 km depth, host brackish waters; (b) the above 1.3–1.4 km thick Upper Triassic to Lower Jurassic carbonate sequences from 1.5–4.5 km depth in the east to 4–6 km depth in the west, contain mainly salty water; (c) the about 1 km thick Middle Jurassic to Lower Cretaceous carbonate contains mainly brackish aquifer. The multichannel seismic profile GT05-07 (Figure 4), offshore Tagliamento river, is located along the slope of the FDCP, where the carbonate sequence is constituted by basinal carbonates and slope (Jurassic-Cretaceous limestones and Upper Cretaceous-Paleocene Scaglia). According to the Amanda 1bis well, the Jurassic-Cretaceous sequences are characterised by a continuous alternation of different salinity waters, while the Upper Cretaceous-Paleocene Scaglia do not appear to host aquifers. The multichannel seismic GT05-09 (Figure 5), offshore Isonzo river, is located on the shelf of the Cretaceous-Paleogene FDCP. These carbonate units host salty and brackish waters, as confirmed by the Grado 1 well, that identified two main fracture zones, from 736 to 740 m and from 1040 to the well bottom at 1108 m, containing low enthalpy (from 30 to 41 °C) salty water, in the Eocene and Cretaceous limestones, respectively [64,76].

(b) The Eocene to Miocene terrigenous units lie above the carbonates: in the basinal area, on the western GT05-07 profile, they are constituted by the Gallare Marls, that in the Amanda 1bis well host brackish waters, while above the FDCP, on the eastern profile GT05-09, these are constituted by the turbiditic terrigenous sequence of the Eocene Trieste Flysch and Miocene Molassa that, in the Grado 1 well, seem to be characterised by low permeability. The top of these units is shaped by the Messinian Unconformity, showing a complex morphology with channels or valleys incised by drainage system (Figures 4 and 5);

(c) The Pliocene progradation sediments, deposited in marine environments on the top of the Messinian Unconformity, according to the Amanda 1bis well, host mainly brackish water;

(d) The early Pleistocene sediments, characterised by marine sediment, deposited from deep to shallow water environments, according to the Amanda 1bis well host salty waters;

(e) The Middle-Late Pleistocene deposits are characterised by the alternation of continental and shallow water sediments related to the cyclicity of glacial and interglacial phases. The base of these units is from 250 to 280 ms twt and from 250–300 ms twt along the lines located near the offshore Tagliamento river and Isonzo river, respectively. In the analysed areas, sediments are mainly composed of silty–clayey fine deposits [28]. The correlation of these sequences with the two hydrogeological transects located near the coast suggests that they host mainly freshwater aquifers identified onshore (Figure 2). The high-resolution single-channel seismic profile APb-F2, offshore the Tagliamento river, and VCT08-12, offshore the Isonzo river (Figure 6) images the last glacial/interglacial cycle.

The lower part of the profiles is constituted by Middle-Late Pleistocene marine sediment deposited during the Thyrrenian transgression (125 ky), probably followed by paralic/transitional sediment. Above them, a high reflective horizon, probably a peat layer, is the base of the Late Pleistocene continental sediments characterised by complex geometries related to the channel levee system, deposited in a fluvial plain environment during the last glacial period, that may host the shallower aquifer A and possibly aquifer B. The Late Pleistocene continental sediments are draped by the prograding Holocene delta front and

pro-delta of the Tagliamento and Isonzo rivers, related to the last marine transgression phase. The high-resolution data show the presence of features that are correlated to fluid seeps coming from the sediment below the high reflective horizon of the probable peat layers. The fluids could be either gas and/or water, and their seeps in the north-eastern Adriatic Sea have been previously recognised, e.g., [77–81].

5. Discussion and Conclusions

The analysed seismic lines image the seismo-stratigraphic sequences that enable us to identify the potential extent of offshore aquifers and their association, with specific sedimentary sequences hosting freshened waters.

The pre-Quaternary lithologies, composed of Middle Triassic to Paleocene carbonate sequences and by Eocene to Pliocene terrigenous sediment, were deposited in marine environments and, on the basis of available data, seem to host waters with variable salinity that are probably ancient marine waters.

On the basis of Amanda 1bis well, the Middle Triassic limestone, probably sealed by the Middle-Upper Triassic terrigenous sediment, could host saline aquifers, while the Upper Triassic to Cretaceous carbonates, overlying the Carnian Unconformity, host an aquifer that is characterised by variability in water salinity content. This variability could be related to the presence of fractures and karstic conduits, strongly influencing fluid circulation. These carbonate sequences experienced subaerial exposures with karstic processes ([48] and references therein), that together with the occurrence of fracture systems, probably related to tectonic phases [47], provide controls for water circulation. This last aquifer is probably sealed by the Cretaceous limestones that pinch out eastward.

In the Eocene and Cretaceous limestones of the FDCP, the presence of the important geothermal aquifer characterised by saline water and intermediate temperatures (from 30 °C to 41 °C, e.g., [64]), could be related to the aquifer system hosted in the several kilometres thick carbonate sequences. The geochemical analysis at the Roman Baths, where the saline water naturally springs, suggests the occurrence of an ancient diagenetically modified paleo-aquifer [65].

The Eocene to Miocene terrigenous units, deposit in marine environments, contain brackish aquifers. Pliocene sediments, underlain by Miocene sediments, fill the paleo-valleys and could host confined freshwater, as already recognised in other areas, e.g., [3]. Onshore, Pliocene and Miocene sediments host the deeper waters of the aquifer system [28], so a continuation in the offshore sediments is a viable hypothesis that is also supported by the sea level decrease that could have triggered an increase in the hydraulic head and steep onshore gradients [82].

The Middle-Late Pleistocene sediments seem to be the only units hosting freshened waters. Firstly, onshore well data confirm the presence of freshwater aquifer systems in proximity to the coastline, supporting the hypothesis of their continuation offshore (Figure 2). Secondly, during the glacial periods, a decrease in sea level (about −120 m with respect to today during the Last Glacial Maximum), provided the total emergence of the northern Adriatic Sea, e.g., [83,84], that represented a fluvial plain, allowing the storage of freshwater. Moreover, a lower sea level position could determine higher groundwater gradients towards offshore areas. On the contrary, during the interglacial ones, the sea level was some meters higher than the present one (about +8 m during the last transgression in the Middle/Late Pleistocene; [85]), with mainly starved conditions. During the deglaciation phases, the fluvial drainage, fed by the melting glaciers, produced the deposition of sediment above the plain. The consequence of these sea level changes is the alternation of terrestrial hosting freshwater aquifers and marine sediment, which could represent impermeable layers separating the aquifers. In addition, the boomer data confirm the fluid circulation of fluid, as shown in Figure 6.

We conclude from our case study that the integration of geological and geophysical data, including in particular seismic imaging, coupled with independent constraints from

wells, can provide a useful approach to unveil the occurrence of potential offshore water reserves providing a foundation for further detailed exploration.

Author Contributions: Conceptualization, M.G. and M.B.; methodology, M.G., M.B., M.D.C., E.B., A.C., G.B. and L.B.; writing—original draft preparation, M.G., M.B., M.D.C. and E.B.; writing—review and editing, M.G., M.B., M.D.C., E.B., A.C., G.B. and L.B.; visualization, M.D.C. and E.B. All authors have read and agreed to the published version of the manuscript.

Funding: This research received no external funding.

Data Availability Statement: The crustal multichannel seismic and exploration well data can be found on the web-based infrastructure "ViDEPI Visibility of Petroleum Exploration Data in Italy (ViDEPI)" (https://www.videpi.com) of the Italian Ministry for Economic Development DGRME, Italian Geological Society, Assomineraria. The water well data are available from the Friuli Venezia Giulia Autonomous Region database (https://www.regione.fvg.it/rafvg/cms/RAFVG/).

Acknowledgments: The authors acknowledge the IHS Markit® that provided the educational licence of the Kingdom™ software for seismic interpretation, the Emerson Paradigm® and the Schlumberger® that provided the Echos™ and Geodepth™ and the Vista® academic licences, respectively, for seismic processing. Thank you very much to Fausto Ferraccioli for his useful advice.

Conflicts of Interest: The authors declare no conflict of interest.

References

1. Custodio, E. Coastal aquifers of europe: An overview. *Hydrogeol. J.* **2010**, *18*, 269–280. [CrossRef]
2. Post, V.E.; Groen, J.; Kooi, H.; Person, M.; Ge, S.; Edmunds, W.M. Offshore fresh groundwater reserves as a global phenomenon. *Nature* **2013**, *504*, 71–78. [CrossRef] [PubMed]
3. Lofi, J.; Inwood, J.; Proust, J.-N.; Monteverde, D.H.; Loggia, D.; Basile, C.; Otsuka, H.; Hayashi, T.; Stadler, S.; Mottl, M.J. Fresh-water and salt-water distribution in passive margin sediments: Insights from integrated ocean drilling program expedition 313 on the New Jersey margin. *Geosphere* **2013**, *9*, 1009–1024. [CrossRef]
4. Lippert, K.; Tezkan, B. On the exploration of a marine aquifer offshore Israel by long-offset transient electromagnetics. *Geophys. Prospect.* **2020**, *68*, 999–1015. [CrossRef]
5. Attias, E.; Thomas, D.; Sherman, D.; Ismail, K.; Constable, S. Marine electrical imaging reveals novel freshwater transport mechanism in Hawai'i. *Sci. Adv.* **2020**, *6*, eabd4866. [CrossRef]
6. Gustafson, C.; Key, K.; Evans, R.L. Aquifer systems extending far offshore on the U.S. Atlantic margin. *Sci. Rep.* **2019**, *9*, 8709. [CrossRef]
7. Micallef, A.; Person, M.; Haroon, A.; Weymer, B.A.; Jegen, M.; Schwalenberg, K.; Faghih, Z.; Duan, S.; Cohen, D.; Mountjoy, J.J.; et al. 3D characterization and quantification of an offshore freshened groundwater system in the Canterbury Bight. *Nat. Commun.* **2020**, *11*, 1372. [CrossRef]
8. Adkins, J.F.; McIntyre, K.; Schrag, D.P. The salinity, temperature and δ18O content of the glacial deep ocean. *Science* **2020**, *298*, 1769–1773. [CrossRef]
9. Cohen, D.; Person, M.; Wang, P.; Gable, C.W.; Hutchinson, D.; Marksamer, A.; Dugan, B.; Kooi, H.; Groen, K.; Lizarralde, D. Origin and extent of fresh paleowaters on the Atlantic continental shelf, USA. *Groundwater* **2010**, *48*, 143–158. [CrossRef]
10. Micallef, A.; Person, M.; Berndt, C.; Bertoni, C.; Cohen, D.; Dugan, B.; Evans, R.; Haroon, A.; Hensen, C.; Jegen, M.; et al. Offshore freshened groundwater in continental margins. *Rev. Geophys.* **2021**, *59*, e2020RG000706. [CrossRef]
11. Hong, W.-L.; Lepland, A.; Himmler, T.; Kim, J.H.; Chand, S.; Sahy, D.; Solomon, E.A.; Rae, J.W.B.; Martma, T.; Nam, S., II; et al. Discharge of meteoric water in the eastern Norwegian Sea since the last glacial period. *Geophys. Res. Lett.* **2019**, *46*, 8194–8204. [CrossRef]
12. Kooi, H.; Groen, J. Geological processes and the management of groundwater resources in coastal areas. *Neth. J. Geosci.* **2003**, *82*, 31–40. [CrossRef]
13. Michael, H.A.; Scott, K.C.; Koneshloo, M.; Yu, X.; Khan, M.R.; Li, K. Geologic influence on groundwater salinity drives large seawater circulation through the continental shelf. *Geophys. Res. Lett.* **2016**, *43*, 10782–10791. [CrossRef]
14. Varma, S.; Michael, K. Impact of multi-purpose aquifer utilisation on a variable-density groundwater flow system in the Gippsland Basin, Australia. *Hydrogeol. J.* **2012**, *20*, 119–134. [CrossRef]
15. Groen, J.; Velstra, J.; Meesters, A. Salinization processes in paleowaters in coastal sediments of Suriname: Evidence from Δ7Cl analysis and diffusion modelling. *J. Hydrol.* **2000**, *234*, 1–20. [CrossRef]
16. Siegel, J.; Person, M.; Dugan, B.; Cohen, D.; Lizarralde, D.; Gable, C.W. Influence of late Pleistocene glaciations on the hydrogeology of the continental shelf offshore Massachusetts, USA. *Geochem. Geophys. Geosyst.* **2014**, *15*, 4651–4670. [CrossRef]
17. Van Geldern, R.; Baier, A.; Subert, H.L.; Kowol, S.; Balk, L.; Barth, J.A.C. Pleistocene paleo-groundwater as a pristine fresh water resource—Evidence from stable and radiogenic isotopes. *Sci. Total Environ.* **2014**, *496*, 107–115. [CrossRef]

18. DeFoor, W.; Person, M.; Larsen, H.C.; Lizarralde, D.; Cohen, D.; Dugan, B. Ice sheet-derived submarine groundwater discharge on Greenland's continental shelf. *Water Resour. Res.* **2011**, *47*, W07549. [CrossRef]
19. Lemieux, J.-M.; Sudicky, E.A.; Peltier, W.R.; Tarasov, L. Simulating the impact of glaciations on continental groundwater flow systems: 1. Relevant processes and model formulation. *J. Geophys. Res.* **2008**, *113*, F03017. [CrossRef]
20. Marksammer, A.J.; Person, M.A.; Day-Lewis, F.D.; Lane, J.W.; Cohen, D.; Dugan, B.; Kooi, H.; Willett, M. Integrating geophysical, hydrochemical, and hydrologic data to understand the freshwater resources on Nantucket Island, Massachusetts. In *Subsurface Hydrology: Data Integration for Properties and Processes*; Hyndman, D.W., Day-Lewis, F.D., Singha, K., Eds.; AGU Water Resources Monograph; American Geophysical Union: Washington, DC, USA, 2007; pp. 143–159.
21. Person, M.; Dugan, B.; Swenson, J.B.; Urbano, L.; Stott, C.; Taylor, J.; Willett, M. Pleistocene hydrogeology of the Atlantic continental shelf, New England. *Geol. Soc. Am. Bull.* **2003**, *115*, 1324–1343. [CrossRef]
22. Person, M.; Marksamer, A.; Dugan, B.; Sauer, P.E.; Brown, K.; Bish, D.; Licht, K.J.; Willett, M. Use of a vertical δ18O profile to constrain hydraulic properties and recharge rates across a glacio-lacustrine unit, Nantucket Island, Massachusetts, USA. *Hydrogeol. J.* **2012**, *20*, 325–336. [CrossRef]
23. Uchupi, E.; Driscoll, N.; Ballard, R.D.; Bolmer, S.T. Drainage of late Wisconsin glacial lakes and the morphology and late Quaternary stratigraphy of the New Jersey-southern New England continental shelf and slope. *Mar. Geol.* **2001**, *172*, 117–145. [CrossRef]
24. Hupers, A.; Kopf, A. Effect of smectite dehydration on pore water geochemistry in the shallow subduction zone: An experimental approach. *Geochem. Geophys. Geosyst.* **2012**, *13*, Q0AD26. [CrossRef]
25. Ijiri, A.; Tomioka, N.; Wakaki, S.; Masuda, H.; Shozugawa, K.; Kim, S.; Khim, B.-K.; Murayama, M.; Matsuo, M.; Inagaki, F. Low-temperature clay mineral dehydration contributes to Porewater dilution in Bering Sea slope subseafloor. *Front. Earth Sci.* **2018**, *6*, 36. [CrossRef]
26. Lin, I.T.; Wang, C.H.; You, C.F.; Lin, S.; Huang, K.F.; Chen, Y.G. Deep submarine groundwater discharge indicated by tracers of oxygen, strontium isotopes and barium content in the Pingtung coastal zone, southern Taiwan. *Mar. Chem.* **2010**, *122*, 51–58. [CrossRef]
27. Zini, L.; Cucchi, F.; Franceschini, G.; Treu, F. Geochemical and hydrological characteristics of the groundwater aquifers in the alluvial plain of Friuli Venezia Giulia. *GORTANIA Atti Museo Friul. Storia Nat.* **2008**, *30*, 5–30.
28. Zini, L.; Calligaris, C.; Treu, F.; Iervolino, D.; Lippi, F. *Risorse Idriche Sotterranee del Friuli Venezia Giulia: Sostenibilità Dell'attuale Indirizzo*; Edizioni Università di Trieste: Trieste, Italy, 2011; p. 89. Available online: http://eventi.regione.fvg.it/redazione/Reposit/Eventi/1481_RISORSE-IDRICHE-risoluzione-media.pdf (accessed on 1 July 2016).
29. Bertoni, C.; Lofi, J.; Micallef, A.; Moe, H. Seismic reflection methods in offshore groundwater research. *Geosciences* **2020**, *10*, 299. [CrossRef]
30. Zampa, L.S. *New Bathymetric Maps of the North East Adriatic Sea*; Busetti, M., Camerlenghi, A., Eds.; Technical Report 05/2020OGS; National Institute of Oceanography and Applied Geophysics-OGS: Sgonico, Italy, 2020.
31. Trobec, A.; Busetti, M.; Zgur, F.; Baradello, L.; Babich, A.; Cova, A.; Gordini, E.; Romeo, R.; Tomini, I.; Poglajen, S.; et al. Thickness of marine Holocene sediment in the Gulf of Trieste (Northern Adriatic Sea). *Earth Syst. Sci. Data* **2018**, *10*, 1077–1092. [CrossRef]
32. EMODnet Bathymetry Consortium. EMODnet Digital Bathymetry. 2018. Available online: https://www.emodnet.eu (accessed on 1 March 2018).
33. IDT-RV Infrastruttura Dati Territoriali della Regione del Veneto. 2017. Available online: https://idt2.regione.veneto.it (accessed on 1 December 2017).
34. IRDAT-FVG. Infrastruttura Regionale di Dati Ambientali e Territoriali per il Friuli Venezia Giulia. 2017. Available online: https://irdat.regione.fvg.it/WebGIS/ (accessed on 1 June 2017).
35. Arso, Ministry of the Environment and Spatial Planning, Slovenian Environment Agency. 2017. Available online: https://gis.arso.gov.si (accessed on 1 April 2017).
36. EU-DEM. Copernicus Land Monitoring Service. 2017. Available online: https://www.eea.europa.eu/data-and-maps/data/copernicus-land-monitoring-service-eu-dem (accessed on 1 July 2017).
37. Ambrosetti, P.; Bosi, C.; Carraro, F.; Ciaranfi, N.; Panizza, M.; Papani, G.; Vezzani, L.; Zanferrari, A. Neotectonic Map of Italy: Scale 1:500,000. Consiglio Nazionale delle Ricerche, Progetto Finalizzato Geodinamica, Sottoprogetto Neotettonica. Litografia Artistica Cartografica, Florence (Italy). 1987. Available online: https://www.socgeol.it/438/structural-model-of-italy-scale-1-500-000.html (accessed on 1 June 2017).
38. Burrato, P.; Poli, M.E.; Vannoli, P.; Zanferrari, A.; Basili, R.; Galadini, F. Sources of M_w 5+ earthquakes in northeastern Italy and western Slovenia: An updated view based on geological and seismological evidence. *Tectonophysics* **2008**, *453*, 157–176. [CrossRef]
39. Cucchi, F.; Piano, C.; Fanucci, C.F.; Pugliese, N.; Tunis, G. *Brevi Note Illustrative della Carta Geologica del Carso Classico Italiano*. 2013, p. 43. Available online: http://www.regione.fvg.it/rafvg/cms/RAFVG/ambiente-territorio/tutela-ambiente-gestione-risorse-naturali/ (accessed on 1 December 2016).
40. Galadini, F.; Poli, M.E.; Zanferrari, A. Seismogenic sources potentially responsible for earthquakes with $M \geq 6$ in the eastern Southern Alps (Thiene–Udine sector, NE Italy). *Geophys. J. Int.* **2005**, *161*, 739–762. [CrossRef]
41. Jurkovšek, B.; Biolchi, S.; Furlani, S.; Kolar-Jurkovšek, T.; Zini, L.; Jež, J.; Tunis, G.; Bavec, M.; Cucchi, F. Geology of the Classical Karst Region (SW Slovenia-NE Italy). *J. Maps* **2016**, *12* (Suppl. S1), 352–362. [CrossRef]

42. Placer, L.; Vrabec, M.; Celarc, B. The bases for understanding of the NW Dinarides and Istria Peninsula tectonics. *Geologija* **2010**, *53*, 55–86. [CrossRef]
43. Zanferrari, A.; Avigliano, R.; Fontana, A.; Paiero, G. Note Illustrative della Carta geologica d'Italia alla scala 1:50,000–Foglio 068 San Vito al Tagliamento. Dipartimento Difesa del Suolo-Servizio Geologico D'Italia. In *Regione Friuli Venezia Giulia-Servizio Geologico*; ISPRA-Servizio Geologico D'italia: Rome, Italy, 2008; p. 178.
44. Cati, A.; Sartorio, D.; Venturini, S. Carbonate Platforms in the Subsurface of the Northern Adriatic Area. *Mem. Soc. Geol. Ital.* **1987**, *40*, 295–308.
45. Zanferrari, A.; Masetti, D.; Monegato, G.; Poli, M.E.; Avigliano, R.; Carraro, F.; Faranda, C.; Grandesso, P.; Ligios, S.; Podda, F.; et al. Carta Geologica d'Italia Alla Scala 1:50,000–Foglio 049 Gemona del Friuli. In *Regione Friuli Venezia Giulia-Servizio Geologico*; ISPRA-Servizio Geologico d'Italia: Rome, Italy, 2013; p. 262.
46. Busetti, M.; Volpi, V.; Barison, E.; Giustiniani, M.; Marchi, M.; Ramella, R.; Wardell, N.; Zanolla, C. Meso-Cenozoic seismic stratigraphy and the tectonic setting of the Gulf of Trieste (Northern Adriatic). *GeoActa* **2010**, *SP3*, 1–14.
47. Busetti, M.; Volpi, V.; Nicolich, R.; Barison, E.; Romeo, R.; Baradello, L.; Brancatelli, G.; Giustiniani, M.; Marchi, M.; Zanolla, C.; et al. Dinaric tectonic features in the Gulf of Trieste (Northern Adriatic). *Boll. Geofis. Teor. Appl.* **2010**, *51*, 117–128.
48. Velić, I.; Tišljar, J.; Matičec, D.; Vlahović, I. Introduzione alla Geologia dell'Istria. In *Guida Alle Escursioni, Proceedings of the 80° Riunione Estiva della Società Geologica Italiana, Trieste, Italy, 6–8 Settembre 2000*; Carulli, G.B., Ed.; Università di Trieste: Trieste, Italy; Società Geologica Italiana: Rome, Italy, 2000; pp. 237–244.
49. Zanferrari, A.; Avigliano, R.; Monegato, G.; Paiero, G.; Poli, M.E.; Barbieri, S.; Calderoni, G.; Carraro, F.; Donegana, M.; Grandesso, P.; et al. Note Illustrative della Carta Geologica d'Italia alla Scala 1:50,000, Foglio 066 Udine. In *Regione Friuli Venezia Giulia-Servizio Geologico*; ISPRA-Servizio Geologico d'Italia: Rome, Italy, 2008; p. 176. [CrossRef]
50. Amadori, C.; Garcia-Castellanos, D.; Toscani, G.; Sternai, P.; Fantoni, R.; Ghielmi, M.; Di Giulio, A. Restored topography of the Po Plain-Northern Adriatic region during the Messinian base-level drop—Implications for the physiography and compartmentalization of the palaeo-Mediterranean basin. *Basin Res.* **2018**, *30*, 1247–1263. [CrossRef]
51. Fantoni, R.; Catellani, D.; Merlini, S.; Rogledi, S.; Venturini, S. La registrazione degli eventi deformativi cenozoici nell'avampaese veneto-friulano. *Mem. Soc. Geol. Ital.* **2002**, *57*, 301–313.
52. Ghielmi, M.; Minervini, M.; Nini, C.; Rogledi, S.; Rossi, M. Late Miocene-Middle Pleistocene sequences in the Po Plain-Northern Adriatic Sea (Italy): The stratigraphic record of modification phases affecting a complex foreland basin. *Mar. Pet. Geol.* **2013**, *42*, 50–81. [CrossRef]
53. Massari, F.; Rio, D.; Serandrei Barbero, R.; Asioli, A.; Capraro, L.; Fornaciari, E.; Vergerio, P.P. The environment of Venice area in the past two million years. *Palaeogeogr. Palaeoclimatol. Palaeoecol.* **2004**, *202*, 273–308. [CrossRef]
54. Zecchin, M.; Tosi, L. Multi-sourced depositional sequences in the neogene to Quaternary succession of the Venice area (northern Italy). *Mar. Pet. Geol.* **2014**, *56*, 1–15. [CrossRef]
55. Zecchin, M.; Busetti, M.; Donda, F.; Dal Cin, M.; Zgur, F.; Brancatelli, G. Plio-Quaternary sequences and tectonic events in the northern Adriatic Sea (Northern Italy). *Mar. Pet. Geol.* **2002**. *under review*.
56. Castiglioni, G.B. The eastern sector of the Italian Alps. In *Quaternary Glaciations. Developments in Quaternary Science*; Gibbard, P., Ehlers, J., Eds.; Elsevier: Amsterdam, The Netherlands, 2004; pp. 209–214.
57. Mancin, N.; Di Giulio, A.; Cobianchi, M. Tectonic vs. climate forcing in the Cenozoic sedimentary evolution of a foreland basin (Eastern South Alpine system, Italy). *Basin Res.* **2009**, *21*, 799–823. [CrossRef]
58. Martelli, G.; Granati, C. The confined aquifer system of Friuli Plain (North Eastern Italy): Analysis of sustainable groundwater use. *G. Geol. Appl.* **2006**, *3*, 59–67. [CrossRef]
59. Giustiniani, M.; Accaino, F.; Picotti, S.; Tinivella, U. Characterization of the shallow aquifers by high-resolution seismic data. *Geophys. Prospect.* **2008**, *56*, 655–666. [CrossRef]
60. Giustiniani, M.; Accaino, F.; Picotti, S.; Tinivella, U. 3D seismic data for shallow aquifers characterisation. *J. Appl. Geophys.* **2009**, *68*, 394–403. [CrossRef]
61. Barison, E.; Brancatelli, G.; Nicolich, R.; Accaino, F.; Giustiniani, M.; Tinivella, U. Wave equation datuming applied to marine OBS data and to land high resolution seismic profiling. *J. Appl. Geophys.* **2011**, *73*, 267–277. [CrossRef]
62. Cimolino, A. Caratterizzazione delle Risorse Geotermiche della Bassa Pianura Friulana (Regione FVG): Progetto Geotermia-grado. Ph.D. Thesis, University of Trieste, Trieste, Italy, 2010.
63. ViDEPI-Project. Visibility of Petroleum Exploration Data in Italy. 2009. Available online: https://www.videpi.com (accessed on 1 December 2019).
64. Cimolino, A.; Della Vedova, B.; Nicolich, R.; Barison, E.; Brancatelli, G. New evidence of the outer Dinaric deformation front in the Grado area (NE Italy). *Rend. Fis. Acc. Lincei* **2010**, *21*, 167–179. [CrossRef]
65. Petrini, R.; Italiano, F.; Ponton, M.; Slejko, F.F.; Aviani, U.; Zini, L. Geochemistry and isotope geochemistry of the Monfalcone thermal waters (northern Italy): Inference on the deep geothermal reservoir. *Hydrogeol. J.* **2013**, *21*, 1275–1287. [CrossRef]
66. Žumer, J. Odkritje podmorskih termalnih izvirov. *Geogr. Obz.* **2004**, *51*, 11–17.
67. Faganeli, J.; Ogrinc, N.; Walter, L.M.; Žumer, J. Modelling Method for SDG Phenomen and SGD Measurements in the Gulf of Trieste. Part B: Geochemical Characterization of the Submarine Spring off IZOLA (Gulf of Trieste, N Adriatic Sea). In *Nuclear and Isotopic Techniques for the Characterization of Submarine Groundwater Discharge in Coastal Zone, IAEA-TECDOC-1595*; International Atomic Energy Agency: Vienna, Austria, 2007; pp. 155–160.

68. Della Vedova, B.; Cimolino, A. *Rendiconto delle Attività Svolte e Piattaforma GIS "GEOTERMIA Nord Adriatico"*; Report Dipartimento di Ingegneria Civile ed Ambientale of University of Trieste: Trieste, Italy; National Institute of Oceanography and Applied Geophysics-OGS: Sgonico, Italy, 2016.
69. Scrocca, D.; Doglioni, C.; Innocenti, F.; Manetti, P.; Mazzotti, A.; Bertelli, L.; D'Offizi, S. Atlante CROP–Profili Sismici a riflessione della crosta italiana. *Mem. Descr. Carta Geol. D'italia* **2013**, *62*, 194.
70. Finetti, I.R. CROP Project: Deep Seismic Exploration of the Central Mediterranean and Italy. In *Atlases in Geoscience 1*; Elsevier Science: Amsterdam, The Netherlands, 2005; p. 779.
71. Brancatelli, G.; Busetti, M.; Dal Cin, M.; Forlin, E. Reprocessing the CROP95-M18 vintage multichannel seismic data acquired in the northern Adriatic Sea: The case of high penetration crustal profile recorded in shallow waters. *Bull. Geophys. Oceanogr.*. *under review*.
72. Dal Cin, M. 3D Velocity Depth Model in the Gulf of Trieste by Means of Tomographic Analysis from Multichannel Seismic Reflection Data. Ph.D. Thesis, University of Trieste, National Institute of Oceanography and Applied Geophysics—OGS, International Centre for Theoretical Physics (ICTP), OGS and ICTP, Trieste, Italy, March 2018. Available online: http://hdl.handle.net/11368/2922569 (accessed on 1 July 2020).
73. Dal Cin, M.; Böhm, G.; Busetti, M.; Picotti, S.; Zgur, F.; Camerlenghi, A. 3D velocity-depth model from multichannel seismic in the Dinaric foredeep of the Gulf of Trieste (Adriatic Sea), at the NE edge of Adria plate. *Tectonophysics* **2022**. *under review*.
74. Picotti, S.; Dal Cin, M.; Böhm, G.; Busetti, M. Evidences of Seismic Flysch Anisotropy in the Gulf of Trieste. In Proceedings of the Conference Proceedings, 24th European Meeting of Environmental and Engineering Geophysics, Porto, Portugal, 9–12 September 2018; 2018, pp. 1–5. [CrossRef]
75. Accaino, F.; Busetti, M.; Böhm, G.; Baradello, L.; Affatato, A.; Dal Cin, M.; Nieto, D. Geophysical investigation of the Isonzo Plain (NE Italy): Imaging of the Dinaric foredeep at the Alpine-Dinaric chain convergence zone. *Ital. J. Geosci.* **2019**, *138*, 202–215. [CrossRef]
76. Della Vedova, B.; Castelli, E.; Cimolino, A.; Vecellio, C.; Nicolich, R.; Barison, E. La valutazione e lo sfruttamento delle acque geotermiche per il riscaldamento degli edifici pubblici. *Rass. Tec. Friuli Venezia Giulia* **2008**, *6*, 16–19.
77. Gordini, E.; Falace, A.; Kaleb, S.; Donda, F.; Marocco, R.; Tunis, G. Methane-Related Carbonate Cementation of Marine Sediments and Related Macroalgal Coralligenous Assemblages in the Northern Adriatic Sea. In *Seafloor Geomorphology as Benthic Habitats*; Harris, P.T., Baker, E.K., Eds.; Elsevier: Amsterdam, The Netherlands, 2012; pp. 183–198.
78. Busetti, M.; Zgur, F.; Vrabec, M.; Facchin, L.; Pelos, C.; Romeo, R.; Sormani, L.; Slavec, P.; Tomini, I.; Visnovich, G.; et al. Neotectonic reactivation of Meso-Cenozoic structures in the Gulf of Trieste and its relationship with fluid seepings. In Proceedings of the 32° Convegno del Gruppo Nazionale di Geofisica della Terra Solida (GNGTS), Trieste, Italy, 19–21 November 2013.
79. Vesnaver, A.; Böhm, G.; Cance, P.; Dal Cin, M.; Gei, D. Windowless Q-factor tomography by the instantaneous frequency. *Geophys. Prospect.* **2020**, *68*, 2611–2636. [CrossRef]
80. Vesnaver, A.; Böhm, G.; Busetti, M.; Dal Cin, M.; Zgur, F. Broadband Q-factor imaging for geofluid detection in the Gulf of Trieste (northern Adriatic Sea). *Front. Earth Sci.* **2021**, *9*, 84. [CrossRef]
81. Vesnaver, A.; Busetti, M.; Baradello, L. Chirp data processing for fluid detection at the Gulf of Trieste (northern Adriatic Sea). *Bull. Geophys. Oceanogr.* **2021**, *62*, 365–386. [CrossRef]
82. Zamrsky, D.; Karssenberg, M.E.; Cohen, K.M.; Marc, F.P.; Bierkens, M.F.P.; Oude Essink, G.H.P. Geological heterogeneity of coastal unconsolidated groundwater systems worldwide and its influence on offshore fresh groundwater occurrence. *Front. Earth Sci.* **2020**, *7*, 339. [CrossRef]
83. Velić, J.; Malvić, T. Depositional conditions during Pliocene and Pleistocene in Northern Adriatic and possible lithostratigraphic division of these rocks (Taložni uvjeri tijekom pliocena i pleistocena u Sjevernom Jadranu te moguća litostratigrafska raščlamba nastalih stijena). *Nafta* **2011**, *62*, 25–38.
84. Vai, G.B.; Cantelli, L. *Litho-Palaeoenvironmental Maps of Italy during the Last Two Climatic Extreme, Map 1—Last Glacial Maximum (22 ± 2 ka cal BP)*; Antonioli, F., Vai, G.B., Eds.; Climex Maps Italy: Bologna, Italy, 2004.
85. Waelbroeck, A.C.; Labeyriea, L.; Michel, E.; Duplessy, J.C.; McManus, J.F.; Lambeck, K.; Balbon, E.; Labracherie, M. Sea-level and deep water temperature changes derived from benthic foraminifera isotopic records. *Quat. Sci. Rev.* **2002**, *21*, 295–305. [CrossRef]